Research Article

Formulation Optimization, Characterization, and Antioxidant Activity of Nanoencapsulated *Clitoria ternatea* Flower Extract

Hafi Luthfi Sanjaya, Bella Putri Maharani, Muhlisin*, Aji Praba Baskara and Zuprizal
Department of Animal Nutrition and Feed Science, Faculty of Animal Science, Universitas Gadjah Mada, Yogyakarta, Indonesia

Ronny Martien
Department of Pharmaceutics, Faculty of Pharmacy, Universitas Gadjah Mada, Yogyakarta, Indonesia

Wulandari
Research Center for Animal Husbandry, National Research and Innovation Agency (BRIN), Bogor, Indonesia

* Corresponding author. E-mail: muhlisin.fapet@ugm.ac.id DOI: 10.14416/j.asep.2026.06.001
Received: 28 November 2025; Revised: 21 January 2026; Accepted: 9 April 2026; Published online: 2 June 2026

Abstract
Clitoria ternatea flower extract (CTE) contains bioactive compounds that can alleviate oxidative stress. Nonetheless, these bioactive compounds exhibit instability and low bioavailability. Nanoencapsulation improves stability and bioavailability. This study aimed to establish the optimal formulation of nanoencapsulated *C. ternatea* flower extract (CTE-N) as a feed additive to mitigate oxidative stress in broiler chickens. A D-optimal mixture design was used to optimize the concentration of chitosan, sodium tripolyphosphate (NaTPP), and CTE by considering the encapsulation efficiency of anthocyanin and flavonol. The optimal formulation obtained was characterized, and its antioxidant activity was measured. The results showed that the optimal CTE-N formulation consisted of 66.67% chitosan, 14.42% NaTPP, and 18.91% CTE, with the encapsulation efficiency of anthocyanin was 21.00±1.85% and flavonol was 12.10±1.36%. CTE-N particles had a nanometric size of 142.2±5.46 nm, a zeta potential of 28.23±0.72 mV, a PDI of 0.45±0.08, and spherical particle morphology. CTE-N exhibited higher antioxidant activity than CTE in the DPPH and ABTS radical scavenging assays, while the H_2O_2 radical scavenging, reducing power assay, and TAC assays showed the opposite results (p-value<0.05). In conclusion, the optimum formulation of CTE-N possesses a nanoscale size, a positive surface charge, good homogeneity, and assay-dependent effects of antioxidant activity.

Keywords: Antioxidants, Characteristics, *Clitoria ternatea* flower extract, D-Optimal, Nanoencapsulation

1 Introduction

Oxidative stress occurs when the production of reactive oxygen species (ROS) exceeds the capacity of the endogenous antioxidant system to neutralize them, hence disrupting the body's redox equilibrium and resulting in oxidative damage [1]. In the poultry industry, modern broiler chickens produced by selective breeding exhibit heightened susceptibility to oxidative stress due to their high metabolic rate [2]. Moreover, intensive production systems subject birds to several stressors, including prolonged photoperiods, infections, and heightened levels of ammonia and dust, which cumulatively lead to oxidative stress [3]. Consequently, the increased production of ROS disrupts the antioxidant balance, weakens gastrointestinal health, reduces performance, and results in significant economic losses [4]. Therefore, antioxidants are crucial for regulating the overproduction of ROS and preventing oxidative damage.

Antioxidants are components that have the ability to prevent or inhibit oxidation and can protect against ROS [5]. Butterfly pea (*C. ternatea* Linn. (CT)) is a plant from the Fabaceae family that has antioxidant activity, which can prevent or protect against oxidative damage [6]. This ability is related to the bioactive compounds contained in the *C. ternatea* flower extract, including flavonol glycosides and anthocyanins [7]. Flavonoids in plant extracts are antioxidant compounds that potentially prevent oxidative stress [8]. However, some bioactive flavonoid compounds are susceptible to degradation or alteration during digestion and storage [9]. In an *in vitro* study of the human digestive system, total anthocyanin concentration can decrease by approximately 42%, and antioxidant activity can be lost by as much as 29% during digestion in the intestine [10]. Under neutral or basic pH conditions in the intestine of broiler chicken, flavylium cations of anthocyanin will transform into unstable hemiketal, chalcone, and quinoidal base forms [11].

Nanoencapsulation is a technique of encasing bioactive compounds within a biopolymer matrix at a nanometric size (1–1000 nm), offering numerous advantages for various applications [12], [13]. Chitosan, a heteropolysaccharide comprising an amino group (C-2) and hydroxyl groups (C-3 and C-6), is a polymer commonly used in nanoencapsulation [14]. Chitosan nanoencapsulation can serve as a good carrier for active compounds due to its several characteristics, including biocompatibility, biodegradability, non-toxicity, and mucoadhesiveness [15]. In the digestive tract, chitosan nanoencapsulation acts as a biological membrane that prevents or slows down the degradation of active compounds and increases the residence time in the intestinal lumen due to chitosan's affinity for the intestinal mucosa [16]. Furthermore, the nanometric scale size of nanoparticles allows the particles to move across various biological barriers toward specific target locations, thereby increasing bioavailability [17].

D-optimal mixture design is a statistical method extensively employed to optimize the most effective combination of components via fitted models [18]. This approach optimizes the determinant of the information matrix, thereby reducing the overall variance of the predicted regression coefficients [19]. D-optimal mixture design has numerous advantages in formulation, such as minimizing the number of experimental runs and statistically identifying interactions among components to address the limitations of existing methods. To the best of our knowledge, there are no reported studies on the nanoencapsulation of *C. ternatea* flower extract utilizing chitosan with a D-optimal mixture design. This study sought to determine the best formulation of CTE-N using a D-optimal mixture design. The best formulation was characterized, and its antioxidant activity was assessed.

2 Materials and Methods

2.1 *Extraction of C. ternatea flower*

Extraction of *C. ternatea* flower was performed using the maceration technique. The dried sample was extracted using a 46.69% ethanol solution at a material-to-solvent ratio of 1:10 and a pH of 3.4 for three days, followed by filtration using filter paper. The resulting filtrate was subsequently evaporated with a rotary evaporator at –55 °C (R-300, Buchi Labortechnik AG, Flawil, Switzerland) and stored at –20 °C (DW-40L262, Haier, Qingdao, China) prior to further application. The CTE used in this study has an anthocyanin and flavonol content of 449.03±4.02 µg/g and 13.62±0.17 mg/g CTE paste extract, respectively.

2.2 *Optimization of nanoencapsulation formulation of CTE-N*

CTE-N consists of CTE, chitosan (Shrimp SHELL extract), and NaTPP (Xilong Scientific, Shantou, China). The process of making CTE-N was carried out by mixing the extract at a concentration of 4% (w/v) with a 0.2% (w/v) chitosan solution. The chitosan solution was obtained by dissolving it in a 1% (v/v) acetic acid (Merck, Darmstadt, Germany) solution. The extract and chitosan solutions were homogenized using a magnetic stirrer at a speed of 700 rpm for 30 minutes. A 0.1% (w/v) NaTPP solution was then slowly added and stirred again with a magnetic stirrer (MS7-H550-S, DLAB, Beijing, China) at 700 rpm for 30 min [20]. The optimization formulation of CTE-N was performed using the D-optimal mixture design (Design Expert trial version 13.0.5.0, Stat-Ease Inc., USA). The upper and lower bounds of each component used in this experiment are presented in Table 1.

Table 1: Upper and lower bounds of the independent variables and the target response of the dependent variable.

Independent variable	Lowest Level	Highest Level
Chitosan (%)	58.82	66.67
NaTPP (%)	13.33	23.53
CTE (%)	17.65	20.00
Dependent variable	**Target**	
Anthocyanin encapsulation efficiency (%)	Maximum	
Flavonol encapsulation efficiency (%)	Maximum	

Optimization formulation of the CTE-N was performed based on the encapsulation efficiency (EE) values of anthocyanins and flavonols from each formulation. Encapsulation efficiency was measured by centrifuging at 10,000 rpm (Centrifuge 5425, Eppendorf AG, Hamburg, Germany) for 20 minutes [21]. The resulting supernatant was then measured for anthocyanin [22] and flavonol [23] content. Encapsulation efficiency is measured using the equation below:

$$\text{EE (\%)} = \frac{\text{Total compound (mg)-total free compound (mg)}}{\text{Total compound (mg)}} \times 100\%$$

2.3 *Characterization of nanoencapsulated C. ternatea flower extract (CTE-N)*

2.3.1 Average hydrodynamic diameter particle size, polydispersity index (PDI), and zeta potential

The average hydrodynamic diameter particle (Z-average), PDI and zeta potential were analyzed using a dynamic light scattering (DLS) (Zetasizer Nano-ZS ZEN3600; Malvern Instruments Ltd., Worcestershire, UK). Disposable cuvettes (Ratiolab GmbH, Dreieich, Germany) were utilized for the assessment of Z-average and polydispersity index, whereas disposable folded capillary cells (DTS1070, Malvern Panalytical, Worcestershire, UK) were employed for the measurement of zeta potential. All measurements were conducted at a temperature of 25 °C. Zetasizer software (version 8.02) was used to calculate the Z-average, PDI, and zeta potential values [24].

2.3.2 Morphology particle

The nanoencapsulated sample was diluted with distilled water at a ratio of 1:5, and a sample drop was stained with 2% phosphotungstic acid for 30 s and placed on a copper grid. The prepared samples were imaged using a TEM (JEM-100 CX, JEOL, Tokyo, Japan) [25].

2.3.3 ATR-FTIR spectroscopy

The samples of CTE-N and CTE were dried using a freeze dryer for 48 hours. ATR-FTIR analysis was performed in the wavenumber range of 400 cm^{-1} to 4000 cm^{-1} [26].

2.4 *Antioxidant activity of nanoencapsulated C. ternatea flower extract (CTE-N)*

The analysis was performed by comparing the antioxidant activity of the CTE-N and the CTE. The antioxidant activity tests conducted included the DPPH radical scavenging activity [27], the ABTS•+ radical scavenging activity [28], reducing power assay [28], H_2O_2 radical scavenging activity [29], and total antioxidant capacity (phosphomolybdenum assay) [28]. Results were expressed as mg of ascorbic acid equivalents g^{-1} CTE-N (mg/g).

2.5 *Statistical analysis*

The D-optimal mixture design was used to determine the optimal formulation between CTE, chitosan, and NaTPP. Statistical parameters used for evaluation included estimation coefficients, lack of fit, and model type. The verification of the optimum formula obtained from the D-optimal mixture design was tested by comparing the predicted values with the actual values using a one-sample T-test [30]. Data of Z-average, zeta potential, PDI, particle morphology, and FTIR were analyzed descriptively. Antioxidant activity data were analyzed using an independent samples T-test. A *p*-value less than 0.05 was considered to be statistically significant. Results were expressed as mean ± standard deviation (SD). Data analysis was performed using OriginPro 2025b version 10.2.5.212.

3 Results And Discussion

3.1 *Optimization formulation of nanoencapsulated C. ternatea flower extract (CTE-N)*

3.1.1 Model fitting

In this study, 16 combinations of independent variables (chitosan, NaTPP, and CTE) were arranged based on the D-optimal design. Based on this

experimental design, the effect of combining chitosan, NaTPP, and CTE on the encapsulation efficiency of anthocyanins and flavonols can be observed in Table 2 below.

Table 2: Effect of variations in the combination of chitosan, NaTPP and CTE based on the D-Optimal design on the encapsulation efficiency of anthocyanins and flavonols.

Composition (%)			Encapsulation efficiency (%)	
Chitosan	**NaTPP**	**CTE**	**Anthocyanin**	**Flavonol**
58.82	23.53	17.65	17.27 ± 0.75	7.65 ± 0.40
58.82	21.18	20.00	17.29 ± 1.54	11.35 ± 0.99
62.75	19.61	17.65	17.66 ± 2.05	12.43 ± 0.65
66.67	13.33	20.00	17.29 ± 1.35	12.72 ± 1.01
62.75	18.43	18.82	17.46 ± 2.05	11.32 ± 1.18
58.82	21.18	20.00	18.36 ± 1.60	10.91 ± 0.57
58.82	23.53	17.65	20.03 ± 0.92	10.32 ± 0.84
64.71	15.88	19.41	19.85 ± 1.45	10.54 ± 0.92
58.82	21.18	20.00	19.40 ± 0.61	11.55 ± 0.60
66.67	13.33	20.00	18.95 ± 0.66	13.06 ± 1.12
66.67	15.69	17.65	18.38 ± 0.75	10.81 ± 0.76
66.67	14.51	18.82	22.32 ± 1.37	13.8 ± 0.56
60.79	20.98	18.24	19.28 ± 1.74	11.92 ± 1.14
66.67	15.69	17.65	19.45 ± 0.98	11.91 ± 1.25
62.75	17.26	20.00	15.65 ± 0.77	13.88 ± 1.58
58.82	22.35	18.82	21.48 ± 1.91	10.49 ± 0.96

The variations in the proportions of chitosan, NaTPP, and CTE influence the encapsulation efficiency of anthocyanins and flavonols. Table 2 shows that chitosan is the primary factor influencing encapsulation efficiency; an increase in chitosan composition correlates with enhanced encapsulation efficiency. The effect of NaTPP is linearly proportional to chitosan, but the encapsulation efficiency exhibits a compound-dependent effect based on varying CTE compositions. Furthermore, the data on the encapsulation efficiency of anthocyanin and flavonol were used to make the model and obtain the optimum formulation. Based on the D-optimal mixture analysis, the model equations presented in Equations (1) and (2) are obtained.

$$Y_1 = 23.1106 * A + 18.8024 * B - 148.69 * C - 16.1661 * AB + 196.276 * AC + 214.683 * BC \quad (1)$$

$$Y_2 = 12.3762 * A + 9.82783 * B + 16.3026 * C \quad (2)$$

Where:
Y_1= anthocyanin encapsulation efficiency
Y_2= flavonol encapsulation efficiency
A= chitosan
B= NaTPP
C= CTE

The results reveal that the anthocyanin encapsulation efficiency is optimally represented by a quadratic model, and the flavonol encapsulation efficiency is best represented by a linear model (Table 3). This result is evidenced by the significant value (p-value < 0.05) in the model type for both dependent variables. This outcome corresponds with the negligible lack of fit for both dependent variables (p-value > 0.05). The lack of fit value pertains to the model's inaccuracy. The adequate precision value for both dependent variables exceeds 4 (Table 3), signifying that the model is applicable in the optimization process to determine the optimal composition for the production of CTE-N.

Table 3: Analysis of variance (ANOVA) of encapsulation efficiency of anthocyanin and flavonol.

	Estimation coefficient	***F*-value**	***p*-value**
Encapsulation efficiency of anthocyanin			
Linear mixture	-	0.67	0.54
A	23.11	-	-
B	18.80	-	-
C	-148.69	-	-
AB	-16.17	10.80	<0.01
AC	196.28	13.46	<0.01
BC	214.68	15.43	<0.01
Lack of fit	-	0.72	0.64
Model type	Quadratic	4.36	0.02
Adeq. precision			8.02
Encapsulation efficiency of flavonol			
Linear mixture	-	5.92	0.02
A	12.38	-	-
B	9.83	-	-
C	16.30	-	-
Lack of fit	-	1.96	0.24
Model type	Linear	5.92	0.02
Adeq. precision			6.71

3.1.2 D-optimal mixture analysis

The encapsulation efficiency of anthocyanins and flavonols rises with an increase in the ratio of chitosan (A) and NaTPP (B) (Figure 1 and Table 3). Our findings align with the prior research of anthocyanin-loaded chitosan nanoparticles, which reported that an increased fraction of chitosan leads to enhanced encapsulation efficiency [31]. Augmenting the chitosan concentration enhances encapsulation efficiency, since a higher quantity of chitosan provides more NH_3^+ groups for binding the active chemical [11]. The combination of chitosan and active compounds yields a chitosan/active compound complex that is generated concurrently [32]. The findings of this study demonstrate that the interaction

effect between the two independent variables, chitosan and NaTPP (AB), significantly (p-value < 0.01) exhibits a negative connection with the encapsulation efficiency of anthocyanin. The inverse connection may arise due to the binding of both NaTPP and bioactive chemicals to the NH_3^+ group in chitosan. At a constant chitosan concentration, an increase in NaTPP concentration results in a diminished proportion of active molecules associated with it. NaTPP binds to chitosan via an electrostatic bond, which is more robust than the hydrogen interaction established between the active chemical and chitosan [33].

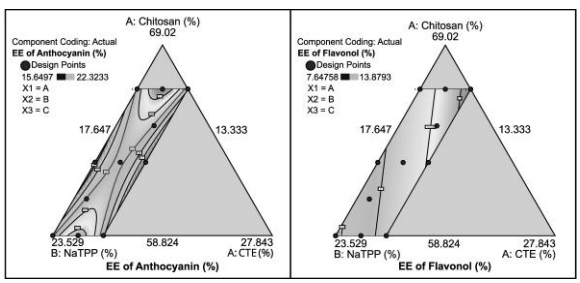

Figure 1: Contour plot of the effect of the combination of chitosan, NaTPP and CTE at different levels on the encapsulation efficiency of anthocyanins and flavonols.

Our finding shows that the proportion of CTE (C) is directly proportional to the encapsulation efficiency of flavonols (-148.69C) and inversely proportional to the encapsulation efficiency of anthocyanins (16.30C). Furthermore, the encapsulation efficiency of anthocyanins is greater than the encapsulation efficiency of flavonols. The greater encapsulation efficiency of anthocyanins compared to flavonols is likely related to the content of hydroxyl groups. The dominant anthocyanin component contained in *C. ternatea* flower extract is delphinidin, while the dominant flavonol component is kaempferol [34]. Delphinidin has a higher number of hydroxyl groups than kaempferol [35], so that more anthocyanins can bind to chitosan. The complex of chitosan and bioactive compounds involves hydrogen bonds formed between the electronegative atoms in the hydroxyl groups of the bioactive compounds and the hydrogen atoms from the amine groups in chitosan ($-NH_3^+$), which are one of the primary forces in nanoparticle formation [36]. Consequently, increasing the proportion of hydroxyl groups can enhance the hydrogen bonding between chitosan and bioactive compounds, thereby improving encapsulation efficiency [37].

The interaction effects of CTE with chitosan (AC) and with NaTPP (BC) both showed significant values (p-value < 0.05) and were positively correlated with anthocyanin encapsulation efficiency. Both types of interactions showed a bimodal distribution pattern in terms of anthocyanin encapsulation efficiency. This pattern suggests that the midpoint of chitosan to CTE or NaTPP to CTE achieves the optimum anthocyanin encapsulation efficiency. However, increasing or decreasing the proportion beyond the midpoint gradually causes a decrease in the anthocyanin encapsulation efficiency. The results of this study are in accordance with previous studies that excessively high anthocyanin concentrations can reduce encapsulation efficiency due to saturation of binding sites in the encapsulant [20], [38]. The formation of the chitosan-anthocyanin complex is contingent upon the concentration of anthocyanin compounds; a larger concentration results in an increased density of hydroxyl groups, hence enhancing the potential for hydrogen bonding with chitosan [39]. However, excessive anthocyanins can saturate the $-NH_3^+$ group on chitosan, resulting in fewer available groups for bonding and hence diminishing encapsulation efficiency [33].

3.1.3 Verification of the optimum formula for nanoencapsulated C. ternatea flower extract (CTE-N)

The D-optimal mixture analysis indicates that the best formulation comprises 66.67% chitosan, 14.42% NaTPP, and 18.91% CTE (Table 4). This formulation was selected because of its better desirability value (0.84) compared to the other alternatives. The selected nanoencapsulation formulation is predicted to achieve an encapsulation efficiency of anthocyanin 21.58% and an encapsulation efficiency of flavonol 12.59%.

Table 4: Ingredients composition of the optimal CTE-N.

Composition (%)			EE (%)		Des
Cth	NaTPP	CTE	Ant	Flav	
66.67	14.42	18.91	21.58	12.59	0.84
58.82	22.13	19.05	21.23	10.72	0.64

Description: Cth: chitosan; CTE= *C. ternatea* flower extract, Ant: anthocyanin; Flav: flavonol; Des: desirability; EE= encapsulation efficiency

The verification procedure involves comparing the predicted values with the actual values acquired from the experiment that are displayed in Table 5. The results of the optimum formulation verification

showed that the encapsulation efficiency values for anthocyanins and flavonols were in the range between the lower 95% PI and the upper 95% PI (Table 5). These results indicate that the previously recommended formula has quite satisfactory quality [40]. Verification was also carried out using a one-sample t-test by comparing the predicted values with the actual values. The analysis results indicated that there was no significant difference (p-value > 0.05) between the predicted and actual values, both in the encapsulation efficiency values of anthocyanins and flavonols. The non-significant difference between the predicted and actual values indicates that the previously created model can be used to develop a formulation according to the targeted objectives [30]. Overall, the results of the study above indicate that the D-optimal mixture design can be used to optimize the nanoencapsulation formulation of CTE-N according to the desired target response.

Table 5: Verification of predicted values with actual values of the formulation.

Variable	Prediction	Actual	*p*-value
EE Ant	21.58	21.00±1.85	0.48
EE Flav	12.59	12.10±1.36	0.42

Description: Ant: anthocyanin; Flav: flavonol; EE= encapsulation efficiency.

3.2 *Characterization of nanoencapsulated C. ternatea flower extract (CTE-N)*

3.2.1 The average hydrodynamic diameter size (Z-average)

The Z-average of the CTE-N obtained in this study was 142.2±5.46 nm (Figure 2). The mean particle size obtained in this study is less than the particle size of nanoencapsulated blueberry (*Vaccinium myrtillus*) extract from previous research, recorded at 504.2 nm [41], and resides within the particle size range of nanoencapsulated extract from *Pandanus tectorius* fruit, which spans from 110.5 to 181.3 nm [42]. The composition of the materials used in the nanoencapsulation process influences the particle size of the nanoencapsulation. The lower the ratio of chitosan to extract, the smaller the particle size [43]. Conversely, the higher the ratio of chitosan to NaTPP, the smaller the particle size [44]. Nanoparticles with small sizes can be formed by adding NaTPP at low concentrations, where both materials will form ionic interactions that bind the active compounds within the system [38].

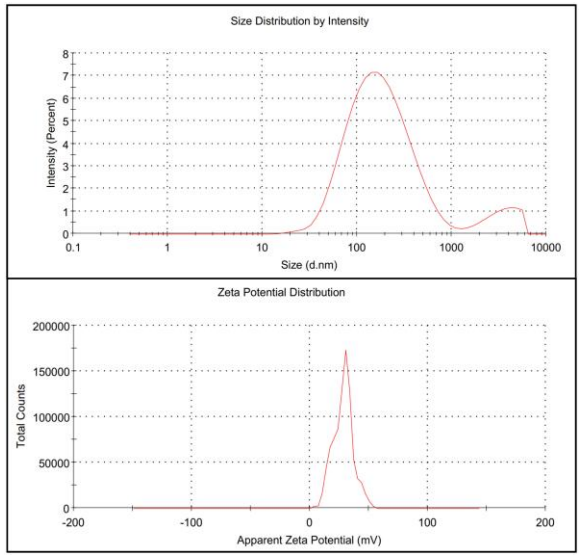

Figure 2: Z-average and zeta potential of CTE-N

3.2.2 Zeta potential

Zeta potential is a parameter that represents the surface electrical charge characteristics of nanoparticles and is related to the electrostatic interactions between particles in a colloidal system [40]. The zeta potential value indicates the attractive or repulsive forces between adjacent particles [44]. The results of this study show that the average zeta potential value is 28.23 ± 0.72 mV. The zeta potential of the nanoencapsulated particles produced in this study is lower than that of nanoencapsulated Maqui extract (*Aristotelia chilensis*) obtained from a previous study, which has a zeta potential value of 33.68 to 41 mV [45], and nanoencapsulated grape water extract, which has a zeta potential value of 24.6 to 35 mV [43]. The zeta potential value of the nanoparticle dispersion obtained in this study falls within the range of ±20 to ±30 mV, which can be classified as having moderate stability [46]. Furthermore, the zeta potential value obtained in this study is positive, which is related to the amine groups present in chitosan [38].

3.2.3 Polydispersity index (PDI)

PDI is the ratio between the average molecular weight and the average number of molecules, representing the uniformity of particle size distribution. A PDI value close to 0 indicates particle size homogeneity, while a PDI value greater than 0.5 indicates a heterogeneous particle size distribution [40]. The results of this study

show a PDI value of 0.45±0.08, indicating that the particle size distribution is still considered homogeneous. The PDI value obtained in this study is higher than the PDI value from prior research of nanoencapsulated Litchi polyphenols, which the PDI value was 0.156 [47]. This study's results confirm the homogeneity of the particle size distribution.

3.2.4 Morphology particles

The nanoparticles in this study had a spherical morphology and a size of ~150 nm (Figure 3). The diameter of the particle obtained from TEM analysis was confirmed using the DLS technique. The morphology of the CTE-N obtained in this study is consistent with the previous study of nanoencapsulated quercetin that has a compact structure and nearly spherical shape [32]. The small particle size and symmetrical morphology of the nanoencapsulated samples indicate an optimum ratio between chitosan and NaTPP [20].

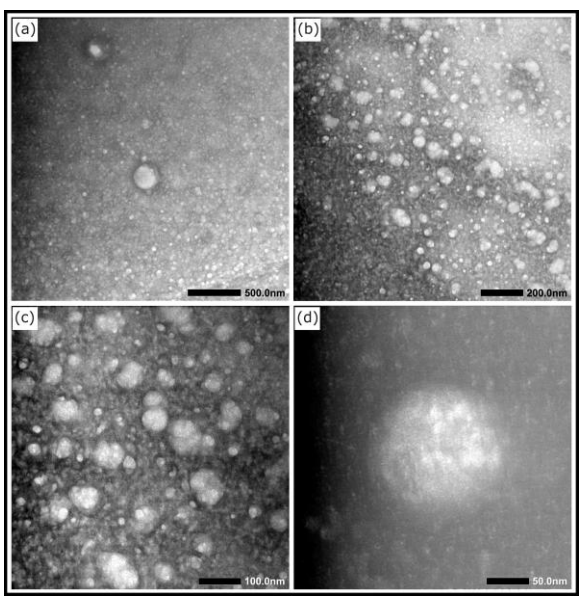

Figure 3: Morphology of CTE-N particle visualized by TEM at different magnifications. (a) 10,000x magnification, (b) 20,000x magnification, (c) 40,000x magnification, (d) 80,000x magnification

3.2.5 ATR-FTIR spectroscopy

Figure 4 illustrates the functional groups present in CTE-N, CTE, chitosan, and NaTPP. The chitosan spectrum exhibits vibrations at 3360 cm^{-1} and 3302 cm^{-1}, corresponding to the stretching of ─OH and N─H groups [44], whereas 2912 cm^{-1} indicates C─H stretching [48]. The spectral peak at 1647 cm^{-1} signifies the presence of a ─$CONH_2$ group from amide I and is linked to the axial deformation of C═O associated with the residual chitin in chitosan [49]. The spectra peak at 1589 cm^{-1} signifies C─N stretching [20], while the peak at 1419 cm^{-1} denotes N─H bending [40]. The peak at 1149 cm^{-1} signifies the stretching of the C─O─C bond in β─1─4 glucose [32]. The C─O stretching of oxygen in the pyran ring is signified by vibrations at 1030 cm^{-1} [50]. The peak at 876 cm^{-1} corresponds to the vibration of the pyranose ring in chitosan [38].

The structural spectrum of NaTPP features vibrations at 1134 cm^{-1}, indicative of the asymmetric stretching of the phosphate group ─PO_2, and a vibration at 887 cm^{-1}, signifying the asymmetric stretching of P─O─P [49]. The FTIR spectra of CTE exhibit a vibration at 3317 cm^{-1}, signifying the presence of a ─OH group [51]. The vibration at 2928 cm^{-1} indicates the presence of C─H stretching [45]. The aromatic ring associated with flavonoid compounds is indicated by a vibration at 1608 cm^{-1} [45], whereas the stretching of the ═C─O─C group within the flavonoid ring is represented by a vibration at 1512 cm^{-1} [38]. The peak at 1404 cm^{-1} indicates vibrations from the bending of the ─CH_3 group, whereas 1030 cm^{-1} denotes the stretching of C─O [44].

CTE-N was identified by the presence of several spectral peaks. After the gelation process, there was a peak shift from 3317 cm^{-1} in CTE-N to 3302 cm^{-1} and a decrease in intensity, indicating a change in hydrogen bonding of the ─OH group [49]. This change in intensity also indicates the presence of intermolecular hydrogen bonds that are likely formed due to cross-linking [26]. A shift in C-H vibrations also occurred, as indicated by a shift from 2912 cm^{-1} in chitosan and 2928 cm^{-1} in CTE to 2924 cm^{-1} in the CTE-N. The peak changes that occur in the range of 1500 cm^{-1}–1600 cm^{-1}, the appearance of a peak at 1558 cm^{-1}, and the absence of a peak at 1647 cm^{-1} in CTE-N indicate that flavonoids enter the encapsulation system. This is because changes in this range are related to the C═C stretching of the aromatic ring [48]. The peak at 1404 cm^{-1} indicates the vibration of the methyl group [44]. Furthermore, a peak shift also occurred from 1030 cm^{-1} in chitosan and CTE to 1022 cm^{-1} in the CTE-N, which is likely related to the C─O stretching of the hydroxyl group of the saccharide [38], [52].

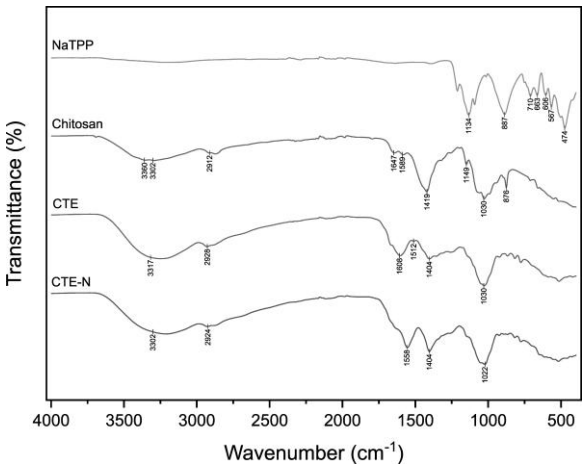

Figure 4: ATR-FTIR spectroscopy of CTE-N and its components.

The features of CTE-N identified in this study demonstrate its appropriateness as a feed additive for broiler chickens. The nanometric size of CTE-N offers advantages, including enhancing the penetration process via the intestinal epithelial cell membrane [53]. Furthermore, the nanometric sizes of the nanoparticles enhance the water solubility of the predominantly hydrophobic extract [54], enabling its administration by drinking water. Moreover, the positive surface charge of the CTE-N particles, shown by the zeta potential value, will interact in electrostatic interactions with the negative charge of the intestinal mucosal surface [55], thus enhancing cellular uptake [56]. Moreover, the bioactive compounds incorporated inside the chitosan nanoencapsulation system, as indicated by FTIR data, can enhance the stability of these compounds, hence extending their shelf life and protecting them from degradation in the digestive tract [57], [58]. However, further research should be carried out to investigate the bioavailability, the stability, and the release kinetics of bioactive compounds from CTE-N, particularly anthocyanins and flavonols.

3.3 *Antioxidant activity of Nanoencapsulated C. ternatea flower extract (CTE-N)*

3.3.1 DPPH radical scavenging activity

In this study, the DPPH test shows that the antioxidant activity of the CTE-N surpasses that of the unencapsulated extract (Figure 5). Our finding aligns with nanoencapsulated grape extract that exhibited superior antioxidant activity in the DPPH assay compared to the extract form [43]. The antioxidant activity of CTE-N and CTE is associated with bioactive compounds, such as anthocyanin ternatin, quercetin, myricetin, and kaempferol [59]. The DPPH free radical scavenging capacity of bioactive components in the extract is associated with the hydroxylation and methoxylation activity in ring B. Delphinidin, characterized by an O-diphenyl structure in ring B, demonstrates significant efficacy in binding DPPH radicals [60]. This study demonstrated that CTE-N exhibited higher antioxidant activity compared to the extract, likely due to enhanced dispersion of hydrophobic substances [61] and the presence of hydroxyl and amine groups in chitosan, which interact with free radicals [43]. However, it is important to point out that unloaded chitosan nanoparticles exhibit restricted antioxidant activity [43], [62], with certain investigations reporting a complete absence of antioxidant activity [63].

3.3.2 ABTS•+ radical scavenging activity

The CTE-N exhibited better antioxidant activity compared to the extract alone (Figure 5). This finding aligns with the nanoencapsulation of buriti oil (*Mauritia flexuosa* L.f.) that exhibited superior antioxidant activity compared to its unencapsulated form [64]. The antioxidant efficacy of CTE-N correlates with the makeup of its bioactive constituents, specifically flavonols and anthocyanins. The 3' and 4' dihydroxyphenyl groups in ring B of polyphenols and flavonoids typically account for their antioxidant activity, as they can generate ortho-semiquinones and subsequently ortho-quinones via two successive single electron transfer processes [65].

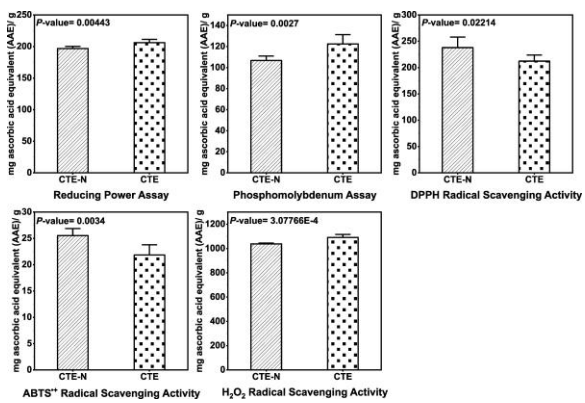

Figure 5: Antioxidant activity of CTE-N and CTE with various types of antioxidant tests.

3.3.3 Reducing power assay

The reducing power assay was performed to assess the electron-donating capacity of the sample, which is crucial to the reduction of Fe^{3+} to Fe^{2+} [66]. Our findings indicate that the CTE-N showed a reduced reduction capacity relative to the unencapsulated extract. Our results contrast with the nanoencapsulation of buriti oil that enhanced the reducing capability [64]. The reducing power assay reflects electron-donating capacity, which is crucial to the reduction of Fe^{3+} to Fe^{2+} [66]. Bioactive substances, including polyphenols and flavonoids, possess hydroxyl groups that function as electron donors [67]. In nanoencapsulation systems, there is a reduction in electron donor capacity, potentially due to steric hindrance [68]. The formation of nanoparticles by electrostatic interactions and chemical crosslinking might alter the local environment of functional groups in polymers, resulting in a denser structure that could cause steric hindrance [68], [69].

3.3.4 H_2O_2 radical scavenging activity

In the metabolic process, H_2O_2 is a molecule generated by the reduction of two electrons from O_2 and the incorporation of $2H^+$. Hydrogen peroxide (H_2O_2) is not a radical chemical; nonetheless, it can be transformed into the hydroxyl radical (HO•) via hemolytic fission, a process facilitated by transition metal ions (Fenton reaction) [70]. Figure 5 shows that the H_2O_2 scavenging activity of CTE-N is lower than that of CTE. Our finding contradicts the prior study of nanoencapsulated curcumin with chitosan that exhibited better scavenging activity against H_2O_2 relative to non-encapsulated curcumin [71]. The diminished scavenging activity of the CTE-N in this study is presumably attributable to the bioactive chemicals enclosed inside the nanoencapsulated particles. The nanoencapsulation potentially inhibits electron or proton (H^+) donors from flavonoids and polyphenols, which are crucial for neutralizing H_2O_2. Our result aligns with previous studies indicating that the capacity to reduce H_2O_2 correlates with phenolic content, which can donate electrons, thereby decomposing H_2O_2 into water [72].

3.3.5 Total antioxidant capacity by phosphomolybdenum assay

Total antioxidant capacity is based on the reduction of the Mo^{6+} ion to Mo^{5+} and the formation of a green phosphate-Mo(V) complex under acidic conditions [73]. The result showed that CTE-N exhibits a reduced total antioxidant capacity relative to CTE (Figure 5). Our finding aligns with a previous study that reported the antioxidant activity of nanoencapsulated anthocyanins is inferior to that of pure, non-encapsulated anthocyanins, due to the entrapment of bioactive compounds within the biopolymer nanoparticles [20]. In this study, the diminished antioxidant activity of CTE-N compared to CTE was likely attributable to the acidic conditions present in the phosphomolybdenum assay. In an acidic environment, the chitosan-TPP nanoparticle complex remains stable, but at physiological pH, the chitosan-TPP complex is entirely dissociated [74]. The acidic pH likely stabilized the chitosan-TPP nanoparticle complex [75], which probably diminished the electron donor capacity of the bioactive compounds within the complex, leading to lowered antioxidant activity values.

4 Conclusions

The optimal formulation for the CTE-N consists of 66.67% chitosan, 14.42% NaTPP, and 18.91% CTE. Particles of CTE-N possess a nanometric particle size, a positive surface charge, and good uniformity in particle size. The CTE-N exhibits assay-dependent effects of antioxidant activity. These characteristics and native antioxidant capacity enable CTE-N to potentially be used as a feed additive to mitigate oxidative stress in broiler chickens.

Acknowledgments

We extend our sincere thanks to the Ministry of Education, Culture, Research and Technology of the Republic of Indonesia for its financial support of the research study via the Pendidikan Magister Menuju Doctor untuk Sarjana Unggul (PMDSU) scholarship with the contract number 018/E5/PG.02.00/PL /2023; 2208/UN1/DITLIT/Dit-Lit/PT.01.03/2023. The authors also acknowledge the Laboratory of Tropical Animal Research Center, Faculty of Animal Science, Universitas Gadjah Mada, for the facilities and assistance during this research.

Author Contributions

The final version of the work was reviewed and approved by all authors. HLS investigation, data curation, data analysis, and writing an original draft. BPM investigation and data curation. M conceptualization, methodology, reviewing and editing. RM methodology and research design. APB research design and data analysis. Z funding acquisition and project administration. W investigation and data curation.

Conflicts of Interest

The authors declare no conflict of interest.

Declaration of generative AI and AI-assisted technologies in the writing process

The authors have not utilised any generative AI tool for any assistance in the writing process.

References

[1] V. Ngo and M. L. Duennwald, "Nrf2 and oxidative stress: A general overview of mechanisms and implications in human disease," *Antioxidants*, vol. 11, no. 12, pp. 1–27, Dec. 2022, doi: 10.3390/antiox11122345.

[2] E. Coudert *et al.*, "Slow and fast-growing chickens use different antioxidant pathways to maintain their redox balance during postnatal growth," *Animals*, vol. 13, no. 7, pp. 1–18, Apr. 2023, doi: 10.3390/ani13071160.

[3] B. Mishra and R. Jha, "Oxidative stress in the poultry gut: Potential challenges and interventions," *Frontiers in Veterinary Science*, vol. 6, no. Mar, pp. 1–5, 2019, doi: 10.3389/fvets.2019.00060.

[4] U. E. Obianwuna *et al.*, "Phytobiotics in poultry: revolutionizing broiler chicken nutrition with plant-derived gut health enhancers," *Journal of Animal Science and Biotechnology*, vol. 15, no. 1, pp. 1–33, Dec. 2024, doi: 10.1186/s40104-024-01101-9.

[5] P. Chaudhary *et al.*, "Oxidative stress, free radicals and antioxidants: Potential crosstalk in the pathophysiology of human diseases," *Frontiers in Chemistry*, vol. 11, pp. 1–24, 2023, doi: 10.3389/fchem.2023.1158198.

[6] P. Chayaratanasin, S. Adisakwattana, and T. Thilavech, "Protective role of *Clitoria ternatea* L. flower extract on methylglyoxal-induced protein glycation and oxidative damage to DNA," *BMC Complementary Medicine and Therapies*, vol. 21, no. 1, Dec. 2021, doi: 10.1186/s12906-021-03255-9.

[7] G. K. Oguis, E. K. Gilding, M. A. Jackson, and D. J. Craik, "Butterfly pea (*Clitoria ternatea*), a cyclotide-bearing plant with applications in agriculture and medicine," *Frontiers in Plant Science*, vol. 10, pp. 1–23, May 2019, doi: 10.3389/fpls.2019.00645.

[8] M. S. Khan, S. Khan, N. Khan, and A. S. Khan, "Dietary sources, classification, biosynthesis, and mechanism of action of flavonoids in combating oxidative stress," in *Role of Flavonoids in Chronic Metabolic Diseases*, , pp. 67–114, 2024, doi: 10.1002/9781394238071.ch3.

[9] A. Naeem *et al.*, "The fate of flavonoids after oral administration: a comprehensive overview of its bioavailability," *Critical Reviews in Food Science and Nutrition*, vol. 62, no. 22, pp. 6169–6186, 2022, doi: 10.1080/10408398.2021.1898333.

[10] Y. Liu *et al.*, "Stability and absorption of anthocyanins from blueberries subjected to a simulated digestion process," *International Journal of Food Sciences and Nutrition*, vol. 65, no. 4, pp. 440–448, 2014, doi: 10.3109/09637486.2013.869798.

[11] Y. Shen *et al.*, "Advanced approaches for improving bioavailability and controlled release of anthocyanins," *Journal of Controlled Release*, vol. 341, pp. 285–299, Jan. 2022, doi: 10.1016/j.jconrel.2021.11.031.

[12] T. K. O. Rosales, N. M. A. Hassimotto, F. M. Lajolo, and J. P. Fabi, "Nanotechnology as a tool to mitigate the effects of intestinal microbiota on metabolization of anthocyanins," *Antioxidants*, vol. 11, no. 3, pp. 1–22, Mar. 2022, doi: 10.3390/antiox11030506.

[13] R. Aryani, M. Wati, E. Maytari, R. A. Nugroho, M. Hetty, and R. Rudianto, "Biosynthesis of silver nanoparticles using *Myrmecodia* sp. bulb extract: in vivo wound healing potency in *Mus musculus* L.," *Applied Science and Engineering Progress*, vol. 19, no. 1, pp. 1–15, 2026, doi: 10.14416/j.asep.2025.06.003.

[14] W. Pongprayoon, T. Siringam, A. Panya, and S. Roytrakul, "Application of chitosan in plant defense responses to biotic and abiotic stresses," *Applied Science and Engineering Progress*, vol. 15, no. 1, pp. 1–10, 2022, doi: 10.14416/j.asep. 2020.12.007.

[15] P. Koirala, P. Bhattarai, J. Sriprablom, R. Zhang, S. Nirmal, and N. Nirmal, "Recent progress of functional nano-chitosan in pharmaceutical and biomedical applications: An updated review," *International Journal of Biological Macromolecules*, vol. 285, pp. 1–13, Jan. 2025, doi: 10.1016/j.ijbiomac.2024.138324.

[16] K. Ahmad, Y. Zhang, P. Chen, X. Yang, and H. Hou, "Chitosan interaction with stomach mucin layer to enhances gastric retention and mucoadhesive properties," *Carbohydrate Polymers*, vol. 333, pp. 1–10, Jun. 2024, doi: 10.1016/j.carbpol.2024.121926.

[17] T. Rahman *et al.,* "Nutritional modulation with chitosan nanoparticles and α-tocopherol enhances growth, health and gut histology in butter catfish (*Ompok pabda*)," *Discover Food*, vol. 5, no. 1, pp. 1–18, Dec. 2025, doi: 10.1007/ s44187-025-00621-1.

[18] J. Musika, C. Kapcum, P. Itthivadhanapong, T. Musika, P. Hanmontree, and S. Piayura, "Enhancing nutritional and functional properties of gluten-free Riceberry rice pasta supplemented with cricket powder using D-optimal mixture design," *Frontiers in Sustainable Food Systems*, vol. 8, pp. 1–13, 2024, doi: 10.3389/fsufs.2024. 1417045.

[19] A. Taromsari and B. G. Tarzi, "Optimization of functional gluten-free cake formulation using rice flour, coconut flour, and xanthan gum via D-Optimal mixture design," *Food Science and Nutrition*, vol. 12, no. 12, pp. 10734–10755, Dec. 2024, doi: 10.1002/fsn3.4523.

[20] N. S. Chatterjee *et al.,* "Nanoencapsulation in low-molecular-weight chitosan improves *in vivo* antioxidant potential of black carrot anthocyanin," *Journal of the Science of Food and Agriculture*, vol. 101, no. 12, pp. 5264–5271, Sep. 2021, doi: 10.1002/jsfa.11175.

[21] S. Gooneh-Farahani, S. M. Naghib, and M. R. Naimi-Jamal, "A novel and inexpensive method based on modified ionic gelation for pH-responsive controlled drug release of homogeneously distributed chitosan nanoparticles with a high encapsulation efficiency," *Fibers and Polymers*, vol. 21, no. 9, pp. 1917–1926, Sep. 2020, doi: 10.1007/s12221-020-1095-y.

[22] J. Li, Z. Li, Q. Ma, and Y. Zhou, "Enhancement of anthocyanins extraction from haskap by cold plasma pretreatment," *Innovative Food Science and Emerging Technologies*, vol. 84, Mar. 2023, doi: 10.1016/j.ifset.2023.103294.

[23] D. Jain, M. Meena, P. Janmeda, C. S. Seth, and J. Arora, "Analysis of quantitative phytochemical content and antioxidant activity of leaf, stem, and bark of *Gymnosporia senegalensis* (Lam.) Loes.," *Plants*, vol. 13, no. 11, Jun. 2024, doi: 10.3390/plants13111425.

[24] H. Kim, C. Song, D. Min, J. Yoo, and J. Choi, "Excipient-free nanotransformation of hydrophilic macromolecules using aqueous counter collision for enhanced bioavailability," *International Journal of Biological Macromolecules*, vol. 279, Nov. 2024, doi: 10. 1016/j.ijbiomac.2024.135416.

[25] Z. Yu, D. Yu, J. Dong, and W. Xia, "Ultrasound-reinforced encapsulation of proanthocyanidin by chitosan-chondroitin sulfate nanosystem," *Food Hydrocolloids*, vol. 132, Nov. 2022, doi: 10. 1016/j.foodhyd.2022.107872.

[26] I. Fierri *et al.,* "Formulation, characterization, and antioxidant properties of chitosan nanoparticles containing phenolic compounds from olive pomace," *Antioxidants*, vol. 13, no. 12, pp. 1–20, Dec. 2024, doi: 10.3390/antiox 13121522.

[27] K. Sarabandi, Z. Akbarbaglu, S. H. Peighambardoust, A. Ayaseh, and S. M. Jafari, "Physicochemical, antibacterial and bio-functional properties of persian poppy-pollen (*Papaver bracteatum*) protein and peptides," *Journal of Food Measurement and Characterization*, vol. 17, no. 5, pp. 4638–4649, Oct. 2023, doi: 10.1007/s11694-023-01980-y.

[28] P. Annadurai, V. Annadurai, M. Yongkun, A. Pugazhendhi, and K. Dhandayuthapani, "Phytochemical composition, antioxidant and antimicrobial activities of *Plecospermum spinosum* Trecul.," *Process Biochemistry*, vol. 100, pp. 107–116, Jan. 2021, doi: 10.1016/ j.procbio.2020.09.031.

[29] P. T. Thompson, V. E. Boamah, and M. Badu, "*In-vitro* antioxidant, antimicrobial and phytochemical properties of extracts from the pulp and seeds of the African baobab fruit (*Adansonia digitata* L.)," *Heliyon*, vol. 10, no. 8,

pp. 1–15, Apr. 2024, doi: 10.1016/j.heliyon.2024.e29660.

[30] T. Ujilestari, R. Martien, B. Ariyadi, N. D. Dono, and Zuprizal, "Self-nanoemulsifying drug delivery system (SNEDDS) of *Amomum compactum* essential oil: Design, formulation, and characterization," *Journal of Applied Pharmaceutical Science*, vol. 8, no. 6, pp. 14–21, Jun. 2018, doi: 10.7324/JAPS.2018.8603.

[31] B. He *et al.*, "Loading of anthocyanins on chitosan nanoparticles influences anthocyanin degradation in gastrointestinal fluids and stability in a beverage," *Food Chemistry*, vol. 221, pp. 1671–1677, Apr. 2017, doi: 10.1016/j.foodchem.2016.10.120.

[32] K. V. Jardim, J. L. N. Siqueira, S. N. Báo, and A. L. Parize, "*In vitro* cytotoxic and antioxidant evaluation of quercetin loaded in ionic cross-linked chitosan nanoparticles," *Journal of Drug Delivery Science and Technology*, vol. 74, pp. 1–9, Aug. 2022, doi: 10.1016/j.jddst.2022.103561.

[33] N. C. Silva, C. Chevigny, S. Domenek, G. Almeida, O. B. G. Assis, and M. Martelli-Tosi, "Nanoencapsulation of active compounds in chitosan by ionic gelation: Physicochemical, active properties and application in packaging," *Food Chemistry*, vol. 463, p. 141129, Jan. 2025, doi: 10.1016/j.foodchem.2024.141129.

[34] K. Kazuma, N. Noda, and M. Suzuki, "Flavonoid composition related to petal color in different lines of *Clitoria ternatea*," *Phytochemistry*, vol. 64, no. 6, pp. 1133–1139, 2003, doi: 10.1016/S0031-9422(03)00504-1.

[35] S. Chen, X. Wang, Y. Cheng, H. Gao, and X. Chen, "A review of classification, biosynthesis, biological activities and potential applications of flavonoids," *Molecules*, vol. 28, no. 13, pp. 1–27, Jul. 2023, doi: 10.3390/molecules28134982.

[36] J. Wang, J. Chen, Y. Jiang, B. Yang, and L. Wen, "Effect of phenolic hydrogen on the formation of chitosan-prenylated flavonoids nanocomplexes," *Food Hydrocolloids*, vol. 168, Dec. 2025, doi: 10.1016/j.foodhyd.2025.111523.

[37] Y. Wang, W. Lu, X. Yang, and H. Zhao, "Polyphenolic nano-encapsulation systems: a review of their formation mechanism, bioavailability, and antioxidant activity," *Journal of Food Measurement and Characterization*, vol. 19, no. 11, pp. 8132–8143, Nov. 2025, doi: 10.1007/s11694-025-03554-6.

[38] Y. A. R. Gaviria, W. D. C. Chacon, K. Cesca, G. C. Leandro, G. A. Valencia, and C. da Costa, "Smart labels based on polyvinyl alcohol incorporated with chitosan nanoparticles loaded with grape extract: Functionality, stability and food application," *International Journal of Biological Macromolecules*, vol. 263, pp. 1–10, Apr. 2024, doi: 10.1016/j.ijbiomac.2024.130513.

[39] M. Homayoonfal, M. Mousavi, H. Kiani, G. Askari, S. Desobry, and E. Arab-Tehrany, "Modifying the stability and surface characteristic of anthocyanin compounds incorporated in the nanoliposome by chitosan biopolymer," *Pharmaceutics*, vol. 14, no. 8, Aug. 2022, doi: 10.3390/pharmaceutics14081622.

[40] F. Astutiningsih, S. Anggrahini, A. Fitriani, and S. Supriyadi, "Optimization of saffron essential oil nanoparticles using chitosan-arabic gum complex nanocarrier with ionic gelation method," *International Journal of Food Science*, vol. 2022, no. 1, pp. 1–14, 2022, doi: 10.1155/2022/4035033.

[41] J. G. Franco, L. C. Cefali, J. A. Ataide, A. Santini, E. B. Souto, and P. G. Mazzola, "Effect of nanoencapsulation of blueberry (*Vaccinium myrtillus*): A green source of flavonoids with antioxidant and photoprotective properties," *Sustainable Chemistry and Pharmacy*, vol. 23, pp. 1–6, Oct. 2021, doi: 10.1016/j.scp.2021.100515.

[42] E. Oksal *et al.*, "*In vitro* and *in vivo* studies of nanoparticles of chitosan-*Pandanus tectorius* fruit extract as new alternative treatment for hypercholesterolemia via Scavenger Receptor Class B type 1 pathway," *Saudi Pharmaceutical Journal*, vol. 28, no. 10, pp. 1263–1275, Oct. 2020, doi: 10.1016/j.jsps.2020.08.017.

[43] S. Soleymanfallah, Z. Khoshkhoo, S. E. Hosseini, and M. H. Azizi, "Preparation, physical properties, and evaluation of antioxidant capacity of aqueous grape extract loaded in chitosan-TPP nanoparticles," *Food Science and Nutrition*, vol. 10, no. 10, pp. 3272–3281, Oct. 2022, doi: 10.1002/fsn3.2891.

[44] N. Shahid *et al.*, "Synthesis and evaluation of chitosan based controlled release nanoparticles for the delivery of ticagrelor," *Designed Monomers and Polymers*, vol. 25, no. 1, pp. 55–63, 2022, doi: 10.1080/15685551.2022.2054117.

[45] D. Andrade *et al.*, "Nanoencapsulation of maqui (*Aristotelia chilensis*) extract in chitosan–tripolyphosphate and chenopodin-based systems," *Antioxidants*, vol. 13, no. 3, pp. 1–18, Mar. 2024, doi: 10.3390/antiox13030273.

[46] S. Bhattacharjee, "DLS and zeta potential - What they are and what they are not?," *Journal of Controlled Release*, vol. 235, pp. 337–351, Aug. 2016, doi: 10.1016/j.jconrel.2016.06.017.

[47] X. Cheng et al., "Effects of a chitosan nanoparticles encapsulation on the properties of litchi polyphenols," *Food Science and Biotechnology*, vol. 32, no. 13, pp. 1861–1871, Nov. 2023, doi: 10.1007/s10068-023-01303-3.

[48] V. A. Pereira, I. N. Q. de Arruda, and R. Stefani, "Active chitosan/PVA films with anthocyanins from *Brassica oleraceae* (Red Cabbage) as Time-Temperature Indicators for application in intelligent food packaging," *Food Hydrocolloids*, vol. 43, pp. 180–188, Jan. 2015, doi: 10.1016/j.foodhyd.2014.05.014.

[49] N. C. da Silva, T. T. de Barros-Alexandrino, O. B. G. Assis, and M. Martelli-Tosi, "Extraction of phenolic compounds from acerola by-products using chitosan solution, encapsulation and application in extending the shelf-life of guava," *Food Chemistry*, vol. 354, pp. 1–9, Aug. 2021, doi: 10.1016/j.foodchem.2021.129553.

[50] T. Nalini, S. K. Basha, A. M. Sadiq, and V. S. Kumari, "Pectin / chitosan nanoparticle beads as potential carriers for quercetin release," *Materials Today Communications*, vol. 33, pp. 1–11, Dec. 2022, doi: 10.1016/j.mtcomm.2022.104172.

[51] N. Zahed, R. Esmaeilzadeh Kenari, and R. Farahmandfar, "Effect of different extraction methods on antioxidant properties and encapsulation efficiency of anthocyanin of pomegranate peel," *Food Science & Nutrition*, vol. 11, no. 7, pp. 3780–3787, Jul. 2023, doi: 10.1002/fsn3.3362.

[52] F. A. S. Hassan, E. F. Ali, N. Y. Mostafa, and R. Mazrou, "Shelf-life extension of sweet basil leaves by edible coating with thyme volatile oil encapsulated chitosan nanoparticles," *International Journal of Biological Macromolecules*, vol. 177, pp. 517–525, Apr. 2021, doi: 10.1016/j.ijbiomac.2021.02.159.

[53] Q. Zhong, J. Zeng, and X. Jia, "Self-assembled aggregated structures of natural products for oral drug delivery," *International Journal of Nanomedicine*, vol. 19, pp. 5931–5949, 2024, doi: 10.2147/IJN.S467354.

[54] K. Dudhat and H. Patel, "Preparation and evaluation of pirfenidone loaded chitosan nanoparticles pulmonary delivery for idiopathic pulmonary fibrosis," *Future Journal of Pharmaceutical Sciences*, vol. 8, no. 1, Dec. 2022, doi: 10.1186/s43094-022-00419-3.

[55] S. Hussain *et al.*, "Chitosan as oral absorption enhancer and inhibitor: A comprehensive review," *Chinese Chemical Letters*, vol. 37, no. 1, pp. 1–11, Jan. 2026, doi: 10.1016/j.cclet.2025.111273.

[56] Y. Herdiana, P. Husni, S. Nurhasanah, S. Shamsuddin, and N. Wathoni, "Chitosan-based nano systems for natural antioxidants in breast cancer therapy," *Polymers (Basel)*, vol. 15, no. 13, pp. 1–28, Jul. 2023, doi: 10.3390/polym15132953.

[57] Y. Zhu *et al.*, "Improving stability and bioavailability of curcumin by quaternized chitosan coated nanoemulsion," *Food Research International*, vol. 174, Dec. 2023, doi: 10.1016/j.foodres.2023.113634.

[58] P. Inthamat and U. Siripatrawan, "Influence of chitosan encapsulation on functionality and stability of astaxanthin nanoemulsion fabricated using high pressure homogenization," *International Journal of Biological Macromolecules*, vol. 303, pp. 1–10, Apr. 2025, doi: 10.1016/j.ijbiomac.2025.140379.

[59] E. J. Jeyaraj, Y. Y. Lim, and W. S. Choo, "Effect of organic solvents and water extraction on the phytochemical profile and antioxidant activity of *Clitoria ternatea* flowers," *ACS Food Science and Technology*, vol. 1, no. 9, pp. 1567–1577, Oct. 2021, doi: 10.1021/acsfoodscitech.1c00168.

[60] M. P. Kähkönen and M. Heinonen, "Antioxidant activity of anthocyanins and their aglycons," *Journal of Agricultural and Food Chemistry*, vol. 51, no. 3, pp. 628–633, Jan. 2003, doi: 10.1021/jf025551i.

[61] P. Sinlapapanya *et al.*, "Ethanolic cashew leaf extract encapsulated in tripolyphosphate–chitosan complexes: characterization, antimicrobial, and antioxidant activities," *Colloids and Interfaces*, vol. 8, no. 5, Oct. 2024, doi: 10.3390/colloids8050052.

[62] M. Soltanzadeh, S. H. Peighambardoust, B. Ghanbarzadeh, M. Mohammadi, and J. M. Lorenzo, "Chitosan nanoparticles as a promising

nanomaterial for encapsulation of pomegranate (*Punica granatum* L.) peel extract as a natural source of antioxidants," *Nanomaterials*, vol. 11, no. 6, Jun. 2021, doi: 10.3390/nano11061439.

[63] S. Bhoopathy, D. Inbakandan, T. Rajendran, K. Chandrasekaran, R. Kasilingam, and D. Gopal, "Curcumin loaded chitosan nanoparticles fortify shrimp feed pellets with enhanced antioxidant activity," *Materials Science and Engineering C*, vol. 120, Jan. 2021, doi: 10.1016/j.msec.2020.111737.

[64] N. S. Morais *et al.*, "Nanoencapsulation of buriti oil (*Mauritia flexuosa* L.f.) in porcine gelatin enhances the antioxidant potential and improves the effect on the antibiotic activity modulation," *PLoS One*, vol. 17, no. 3, pp. 1–24, Mar. 2022, doi: 10.1371/journal.pone.0265649.

[65] R. Mattioli, A. Francioso, L. Mosca, and P. Silva, "Anthocyanins: A comprehensive review of their chemical properties and health effects on cardiovascular and neurodegenerative diseases," *Molecules*, vol. 25, no. 17, pp. 1–42, Sep. 2020, doi: 10.3390/molecules25173809.

[66] J. R. dos Santos, D. A. Sabry, G. L. Sassaki, and H. A. O. Rocha, "Gallic acid functionalization improves the pharmacological profile of fucoidan B: A polysaccharide with antioxidant properties," *Polysaccharides*, vol. 6, no. 4, p. 89, Oct. 2025, doi: 10.3390/polysaccharides6040089.

[67] R. C. Lasagas, C. Liang, X. T. H. Luong, and F. Ballesteros, "Reductive degradation of carbon tetrachloride using tree leaf polyphenol-iron complexes for groundwater remediation," *RSC Advances*, vol. 15, no. 28, pp. 22915–22929, Jul. 2025, doi: 10.1039/d5ra01391g.

[68] Y. Chen, J. Xue, and Y. Luo, "Encapsulation of phloretin in a ternary nanocomplex prepared with phytoglycogen–caseinate–pectin via electrostatic interactions and chemical cross-linking," *Journal of Agricultural and Food Chemistry*, vol. 68, no. 46, pp. 13221–13230, Nov. 2020, doi: 10.1021/acs.jafc.9b07123.

[69] W. N. El-Sayed and R. F. M. Elshaarawy, "*Origanum syriacum* oil-loaded carboxymethyl chitosan polyelectrolyte nanoparticles: Box–Behnken design optimization of nano-encapsulation, physicochemical, and therapeutic properties," *Polymer Bulletin*, vol. 82, no. 8, pp. 3321–3351, Jun. 2025, doi: 10.1007/s00289-025-05650-5.

[70] G. Martemucci, C. Costagliola, M. Mariano, L. D'andrea, P. Napolitano, and A. G. D'Alessandro, "Free radical properties, source and targets, antioxidant consumption and health," *Oxygen*, vol. 2, no. 2, pp. 48–78, Jun. 2022, doi: 10.3390/oxygen2020006.

[71] L. Pathak, A. Kanwal, and Y. Agrawal, "Curcumin loaded self assembled lipid-biopolymer nanoparticles for functional food applications," *Journal of Food Science and Technology*, vol. 52, no. 10, pp. 6143–6156, Oct. 2015, doi: 10.1007/s13197-015-1742-2.

[72] A. Richards and S. Chaurasia, "Antioxidant activity and reactive oxygen species (ROS) scavenging mechanism of *Eriodictyon californium*, an edible herb of North America," *Journal of Chemistry*, vol. 2022, pp. 1–8, 2022, doi: 10.1155/2022/6980121.

[73] T. M. Asha and M. R. Prathapachandra Kurup, "An insight into the potent antioxidant activity of a dithiocarbohydrazone appended cis-dioxidomolybdenum (VI) complexes," *Applied Organometallic Chemistry*, vol. 34, no. 9, Sep. 2020, doi: 10.1002/aoc.5762.

[74] P. Mazancová, V. Némethová, D. Treľová, L. Kleščíková, I. Lacík, and F. Rázga, "Dissociation of chitosan/tripolyphosphate complexes into separate components upon pH elevation," *Carbohydrate Polymers*, vol. 192, pp. 104–110, Jul. 2018, doi: 10.1016/j.carbpol.2018.03.030.

[75] C. E. Echeverri-Cuartas, C. Gartner, and Y. Lapitsky, "PEGylation and folate conjugation effects on the stability of chitosan-tripolyphosphate nanoparticles," *International Journal of Biological Macromolecules*, vol. 158, pp. 1055–1062, Sep. 2020, doi: 10.1016/j.ijbiomac.2020.04.118.